

Satellite Measurements of Tropospheric Column O₃ and NO₂ in Eastern and Southeastern Asia: Comparison with a Global Model (MOZART-2)

X. Tie · S. Chandra · J. R. Ziemke · C. Granier ·
G. P. Brasseur

Received: 7 April 2006 / Accepted: 28 August 2006
© Springer Science + Business Media B.V. 2006

Abstract Satellite measurements of tropospheric column O₃ and NO₂ in eastern and southeastern Asia are analyzed to study the spatial and seasonal characteristics of pollution in these regions. Tropospheric column O₃ is derived from differential measurements of total column ozone from Total Ozone Mapping Spectrometer (TOMS), and stratospheric column ozone from the Microwave Limb Sounder (MLS) instrument on the Upper Atmosphere Research Satellite (UARS). The tropospheric column NO₂ is measured by Global Ozone Monitoring Experiment (GOME). A global chemical and transport model (Model of Ozone and Related Chemical Tracers, version 2; MOZART-2) is applied to analyze and interpret the satellite measurements. The study, which is based on spring, summer, and fall months of 1997 shows generally good agreement between the model and satellite data with respect to seasonal and spatial characteristics of O₃ and NO₂ fields. The analysis of the model results show that the industrial emission of NO_x (NO+NO₂) contributes about 50%–80% to tropospheric column NO₂ in eastern Asia and about 20%–50% in southeastern Asia. The contribution of industrial emission of NO_x to tropospheric column O₃ ranges from 10% to 30% in eastern Asia. Biomass burning and lightning NO_x emissions have a small effect on tropospheric O₃ in central and eastern Asia, but they have a significant impact in southeastern Asia. The varying effects of NO_x on tropospheric column ozone are attributed

X. Tie (✉) · G. P. Brasseur
National Center of Atmospheric Research, Boulder, CO, USA
e-mail: xxtie@ucar.edu

S. Chandra · J. R. Ziemke
University of Maryland Baltimore County (UMBC) Goddard
Earth Sciences and Technology (GEST), Baltimore, MD, USA

S. Chandra · J. R. Ziemke
NASA Goddard Space Flight Center, Code 613.3, Greenbelt, MD, USA

C. Granier
NOAA, Boulder, CO, USA

G. P. Brasseur
Max Planck Institute of Meteorology, Hamburg, Germany

to differences in relative abundance of volatile organic compounds (VOCs) with respect to total nitrogen in the two regions.

Key words ozone and NO_2 in Asia · TOMS/MLS · GOME · MOZART-2

1 Introduction

Tropospheric ozone is a key constituent of the global environment. First, it plays an important role in controlling the oxidizing capacity of the atmosphere, and hence the lifetime of reactive atmospheric pollutants. Second, it can have damaging effects on the biosphere (e.g., crop productivity) and on human health. Third, it contributes to 'greenhouse warming'. Nitrogen oxides ($\text{NO}_x = \text{NO} + \text{NO}_2$) are atmospheric catalysts which are closely related to ozone and hydroxyl radicals (Crutzen 1970; Thompson 1992; Seinfeld and Pandis 1998). The abundance of NO_x largely regulates the atmospheric oxidizing power (Vitousek et al. 1997). In the troposphere, NO_x is closely related to the ozone chemistry via two separate processes. Ozone is produced photochemically by the oxidation of carbon monoxide, methane, and volatile organic compounds (VOCs) with presence of the NO_x ($\text{NO} + \text{NO}_2$). Nitrogen oxides are also intricately linked to the hydroxyl radical OH, another key atmospheric oxidizing species. The reaction between NO_2 and OH leads to the formation of relatively stable nitric acid (HNO_3), which can be removed from the atmosphere by precipitation and hence provides important fixed nitrogen for the biosphere.

Nitrogen oxides are emitted into the atmosphere from natural and anthropogenic sources, i.e., from fossil fuel, biomass burning, biofuel, oxidation of atmospheric ammonia, soil, and lightning (Seinfeld and Pandis 1998). In eastern and southeastern Asia, especially China which is undergoing major economic changes, there have been heightened energy usages and significant increases in pollutant emissions including NO_x . The rapid increase in NO_x emissions in Asia has a potential impact on tropospheric ozone concentrations over Asia and other regions of the world. For example, Jacob et al. (1999) shows that the ozone increases by 5% to 10% in the western United States as a result of long range transport of air pollution from China.

A clear understanding of these effects can only be achieved by combining global measurements of tropospheric ozone, NO_x , and other trace constituents with global models of atmospheric chemistry and transport under different conditions. With recent availability of satellite measurements and advancement in the development of global models, such studies have become feasible (e.g., Velders et al. 2001; Chandra et al. 2003; Valks et al. 2003; Kunhikrishnan et al. 2004, Chandra et al. 2004). Kunhikrishnan et al. (2004) studied the spatial and seasonal characteristics of NO_x in the troposphere over Asia using satellite measurements of NO_2 columns (TNO_2) from Global Ozone Monitoring Experiment (GOME) and a global model of atmospheric transport and chemistry. Their study showed that tropospheric ozone in the Indian region is not very sensitive to changes in NO_x emissions. Kunhikrishnan et al. (2004) did not include tropospheric ozone measurements in their study to validate this conclusion. Chandra et al. (2004) compared the satellite measurements of tropospheric column O_3 (TO_3) with TO_3 calculated from a global model called MOZART-2 (Horowitz et al. 2003) in the Northern Hemisphere during spring and summer months. The satellite measurements of TO_3 were obtained from differential measurements of total column ozone from Total Ozone Mapping Spectrometer (TOMS) and stratospheric column ozone from the Microwave Limb Sounder (MLS) on the Upper Atmosphere Research Satellite (UARS). The model results were then analyzed to estimate

the relative importance of surface NO_x emission, lightning NO_x , and stratospheric flux. Chandra et al. (2004) did not include satellite measurements of NO_2 column in their study.

Satellite measurements of TO_3 outside the tropics, based on TOMS/MLS measurements, are available for about 20 months (September 1991–April 1993) during the Nimbus-7 TOMS lifetime and for about two years (August 1996 to mid-1998) during the Earth Probe (EP) TOMS. The latter period overlaps with the TNO_2 measurements from GOME (Burrows et al. 1999). The purpose of this paper is to combine these measurements to characterize the spatial and seasonal distributions of TO_3 and TNO_2 over the eastern and southeastern regions of the Asian continent and compare them with the MOZART-2 model results. The model is subsequently used to evaluate the impact of different types of NO_x emissions affecting both TO_3 and TNO_2 fields. In this study we will limit our comparison to the 1997 period where TO_2 and TNO_2 measurements from EP-TOMS, UARS-MLS, and GOME overlap. 1997 was an El Niño year with a significant change in the convection pattern in the Pacific region, and large scale burning in the Indonesian region by uncontrolled wild fires in the tropical rainforests of Sumatra and Borneo (e.g., Chandra et al. 1998; Hauglustaine et al. 1999; Thompson et al. 2001). The implications of tropospheric ozone changes in the tropics during the 1997 El Niño have been analyzed by Sudo and Takahashi (2001) and Chandra et al. (2002) using global models. We will examine some of the implications of the 1997 El Niño, especially the Indonesian wildfires using the MOZART-2 global model. In Sections 2 and 3 we briefly describe the satellite data and the MOZART-2 global model. Sections 4 and 5 present an analysis of the satellite and model results. Finally, Section 6 summarizes the results of this study.

2 Satellite Data

The methodology for deriving tropospheric column ozone (TO_3) from differential measurements of total column ozone from TOMS, and stratospheric column ozone from the MLS instrument on UARS as discussed in Chandra et al. (2003). The frequency of MLS measurements also changes from almost daily measurements during the Nimbus-7 period to only a few days per month (5–10 days) during the EP TOMS period. The MLS measurements outside $\pm 34^\circ$ latitude are available around every alternate month on average because of a 57° inclination of the UARS orbit and planned rotation of the satellite through yaw about every 36 days (Reber 1993). Because the MLS instrument does not measure ozone below 100 hPa, zonal maps of stratospheric TO_3 are most reliable between $\pm 30^\circ$ latitude where tropopause pressure is close to 100 hPa. In this latitude region the TOMS/MLS residual can be used to derive TO_3 with only minor adjustments for tropopause pressure. Outside $\pm 30^\circ$ latitude, the tropopause pressure increases rapidly to 250–300 hPa towards high latitudes (50° – 60°) with peak values during spring months in both hemispheres. As a result, TOMS/MLS residual has a significant contribution from the stratosphere which is a function of latitude and season. To account for the change in tropopause height, Chandra et al. (2003) developed an empirical correction based on ozonesonde measurements. Using this empirical correction, useful estimates of TO_3 can still be made up to about 50°N after making appropriate adjustments for changes in tropopause pressure, particularly for summer months (Chandra et al. 2003). For World Ozone and Ultraviolet Radiation Data Centre (WOUDC) sonde sites between 20°N and 50°N , the relative bias (TOMS/MLS minus ozonesonde TO_3) and RMS difference between TOMS/MLS and WOUDC TO_3 are respectively -5 DU and 9.1 DU. These values are reduced to 0.2 DU and 5.1 DU when only May–August data are used in calculations.

The GOME instrument on the European ERS-2 satellite was launched in April 1995 and has been operational since July of that year (Burrows et al. 1999). ERS-2 is a sun-synchronous satellite with an equatorial crossing at 10:30 A.M. local time. The GOME spectrometer measures radiances between 232 and 793 nm with a spectral resolution of 0.2 nm below 400 nm and 0.33 nm above 400 nm respectively. (Richters and Burrows 2002, and references therein). The NO₂ column is derived from the spectral analysis of radiances between 423 and 451 nm using a nadir scan with 40 by 320 km² footprint. The accuracy of the NO₂ columns is limited by the uncertainties in tropospheric light path, presence of clouds, and several algorithmic issues related to the assumptions of air mass factor and zonal homogeneities of stratospheric column of NO₂. It is difficult to quantify the overall uncertainty in TNO₂ measurements from GOME and may be as much as 50% (Velders et al. 2001; Richters and Burrows 2002).

3 Global Chemical Transport Model

A global chemistry and transport model (MOZART-2) was developed at the Atmospheric Chemistry Division (ACD) of the National Center for Atmospheric Research (NCAR), in cooperation with the National Oceanic and Atmospheric Administration (NOAA), the Geophysical Fluid Dynamics Laboratory (GFDL), and the Max Planck Institute of Meteorology. MOZART-2 simulates the distribution of tropospheric ozone and its chemical precursors. In its standard configuration it calculates the concentrations of 63 chemical species from the surface up to the middle stratosphere. The model can use meteorological inputs derived either from a general circulation model or from a meteorological reanalysis. MOZART-2 is described in detail by Horowitz et al. (2003). That paper includes an extensive evaluation of MOZART-2, including a comparison of the calculated concentrations with measurements from surface networks (CO and O₃), global O₃ sonde data, and measurements from aircraft (O₃, CO, NO_x, PAN, HNO₃, various RH, CH₂O, etc.). Emissions are based on the global EDGAR v3.0 inventory for 1997 (Olivier et al. 2003) with seasonal variation. The biomass burning emission takes into account for the fire information from satellite measurements during 1997 (Granier et al. 2005). The model sources of NO_x consist of 4 TgN/y from lightning, 0.6 TgN/y from aircraft emission, and 40.79 TgN/y from surface emissions. The latter consists of emissions from industry/fossil fuel (23.11 TgN/y), biomass burning (9.81 TgN/y), biogenic/soil (6.62 TgN/y), and biofuel combustion (1.25 TgN/y). In this study we use dynamical fields provided by the analysis of the European Center for Medium-range Weather Forecast (ECMWF) as model input. The model is integrated from January 1996 to December 1997 with the results obtained between January 1997 and December 1997 used for this study. It is noted that the assimilation winds (ECMWF) and biomass burning emission, which is constrained by satellite data, are consistent with the 1997 El Nino.

4 Characterizations of TO₃ and TNO₂ Fields

In this study we are focusing on the region between 20°S and 50°N in latitude, and 90°E and 150°E in longitude. It covers eastern Asia which includes some heavy industrial emission areas, such as eastern China, Japan, and South Korea, and southeastern Asia which encompasses some important biomass burning areas such as Vietnam, Laos, and Indonesia. The southeastern Asian region is also a region of strong lightning activities

(Bond et al. 2002). All these activities have significant impact on tropospheric ozone and NO_2 . Figure 1a shows TO_3 fields from TOMS/MLS for April, July, and September 1997. These months represent spring, summer, and fall conditions in the Northern Hemisphere. They are chosen because of the availability of TO_3 data north of 30° latitude in these months. As discussed in Section 2, TO_3 measurements outside $\pm 30^\circ$ latitude are available every alternate month on average. Figure 1a shows several interesting features in TOMS/MLS TO_3 including: (1) a plume structure emanating from industrial regions of eastern China and Japan and traversing over the Pacific Ocean; this plume is particularly strong in summer months (July, middle panel) with TO_3 values in the 50–60 DU range, (2) elevated values of TO_3 (~35–40 DU) in the Indonesian region in September (lower panel) associated with uncontrolled fires in the tropical rainforests of Sumatra and Borneo (Chandra et al.

Figure 1 **a** The TOMS/MLS measured TO_3 in DU (Dobson Unit; $1\text{DU} = 2.69 \times 10^{16} \text{molecules} - \text{cm}^{-2}$) in eastern and southeastern Asia in April, July, and September 1997, respectively. **b** Same as Figure 1a except for the MOZART-2 calculated TO_3 . **c** Same as Figure 1a except for the differences (DU) between TOMS/MLS and MOZART-2.

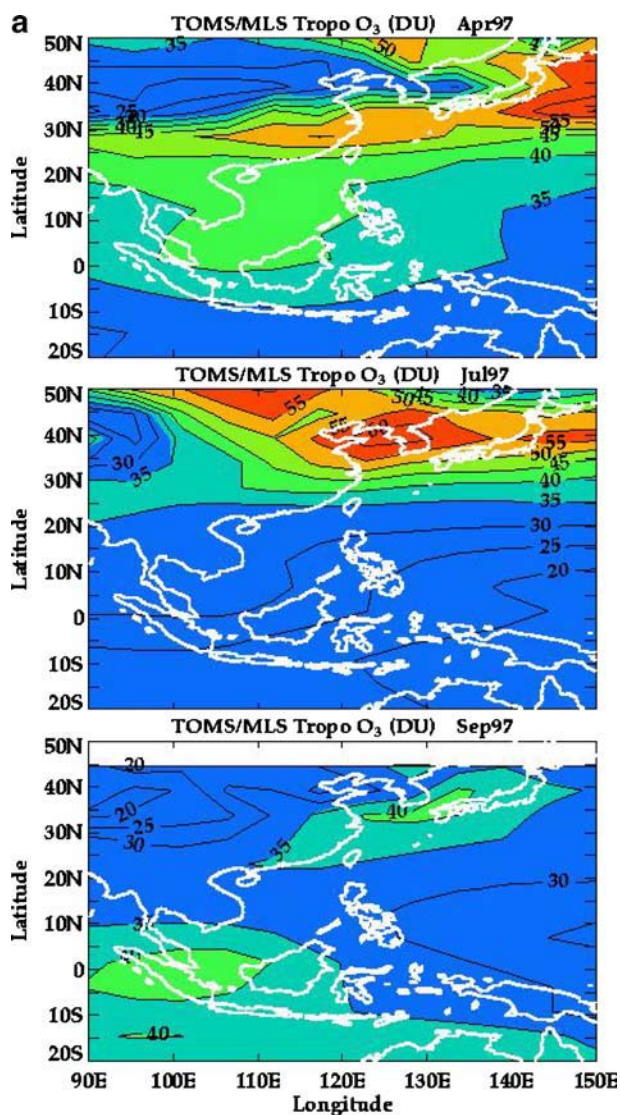
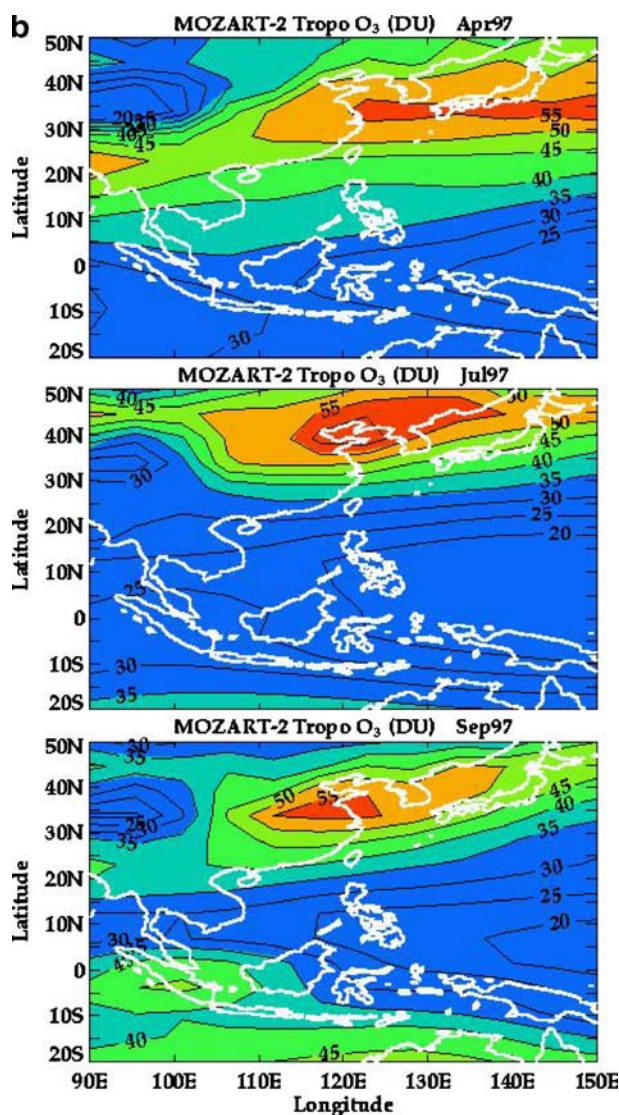


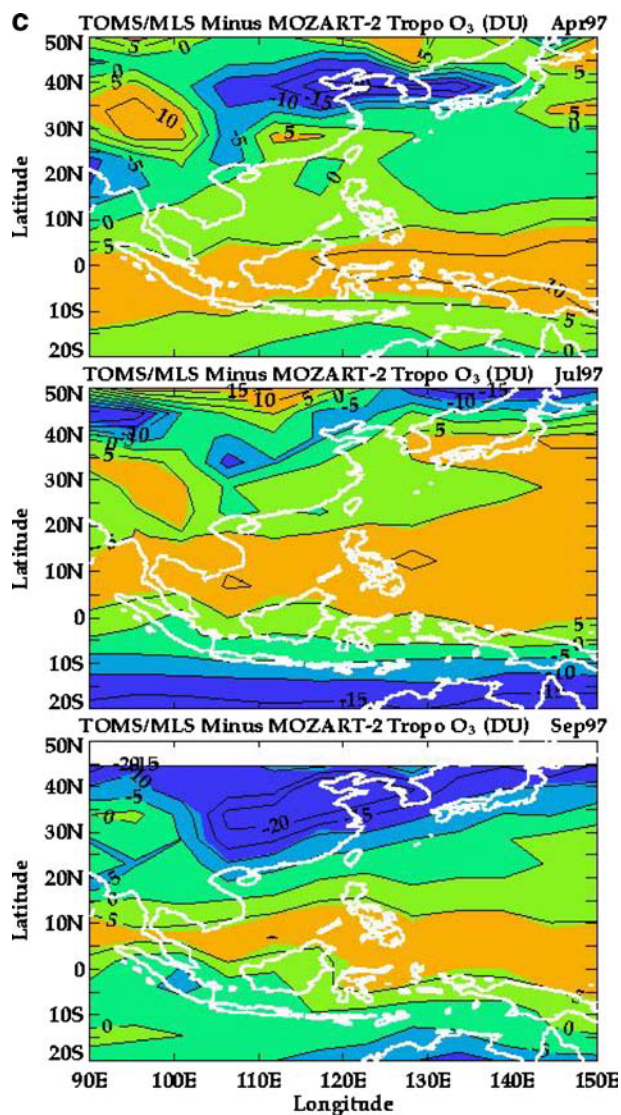
Figure 1 (Continued).



1998; Hauglustaine et al. 1999; Thompson et al. 2001), and (3) a change in seasonal characteristics of TO₃ from south to north with a spring (April) maximum over subtropical latitudes (10–25°N). (The TO₃ values in this latter region vary from 35–45 DU in April to about 30–35 DU in July; north of 30° the seasonal behavior changes to a summer maximum with summer (July) values reaching 55–60 DU.)

The MOZART-2 model captures important features of TO₃ observed by TOMS/MLS as shown in Figure 1b. The simulated plume of TO₃ which originates in eastern China in April is very similar to the observations. In July this plume moves northward to east-central China and is transported into the Pacific. This is also consistent with the observations. In September the high TO₃ calculated by MOZART-2 over Indonesia is also present in the

Figure 1 (Continued).



measurements. However, there are notable differences between measured and calculated TO₃ fields as illustrated by the difference plots in Figure 1c (shown for each month, April, July, and September). For example, the calculated plume structure emanating from eastern China and traversing over the Pacific Ocean is overestimated by about 20 DU in April and September. In general the modeled and observed differences in TO₃ are in the range of 5–10 DU. It is difficult to assess the statistical significance of this difference. Recognizing an uncertainty of about 5 DU in TOMS/MLS measurements based on ozonesonde comparisons, and model uncertainty associated with estimates of surface emissions, meteorological fields, and stratospheric–tropospheric exchange (STE), a difference of 5–10 DU between model and observation is probably not significant. Using this criterion, the modeled and observed values of TO₃ are generally in good agreement except at higher

latitudes in April and September where TOMS/MLS values may be in error (Chandra et al. 2004).

Figure 2 compares column NO_2 retrieved from GOME (left panels) with calculated values from MOZART-2 (right panel) for four selected months (April, July, September, and November) in 1997. The first three months (April, September, and July) are the same as in Figure 1a and b. There are several interesting features in the GOME-measured TNO_2 . For example, there are high amounts of NO_2 located on the east coast of China, South Korea, and Japan with values $\sim 40\text{--}50 \times 10^{14}$ molecules- cm^{-2} . These large column values are

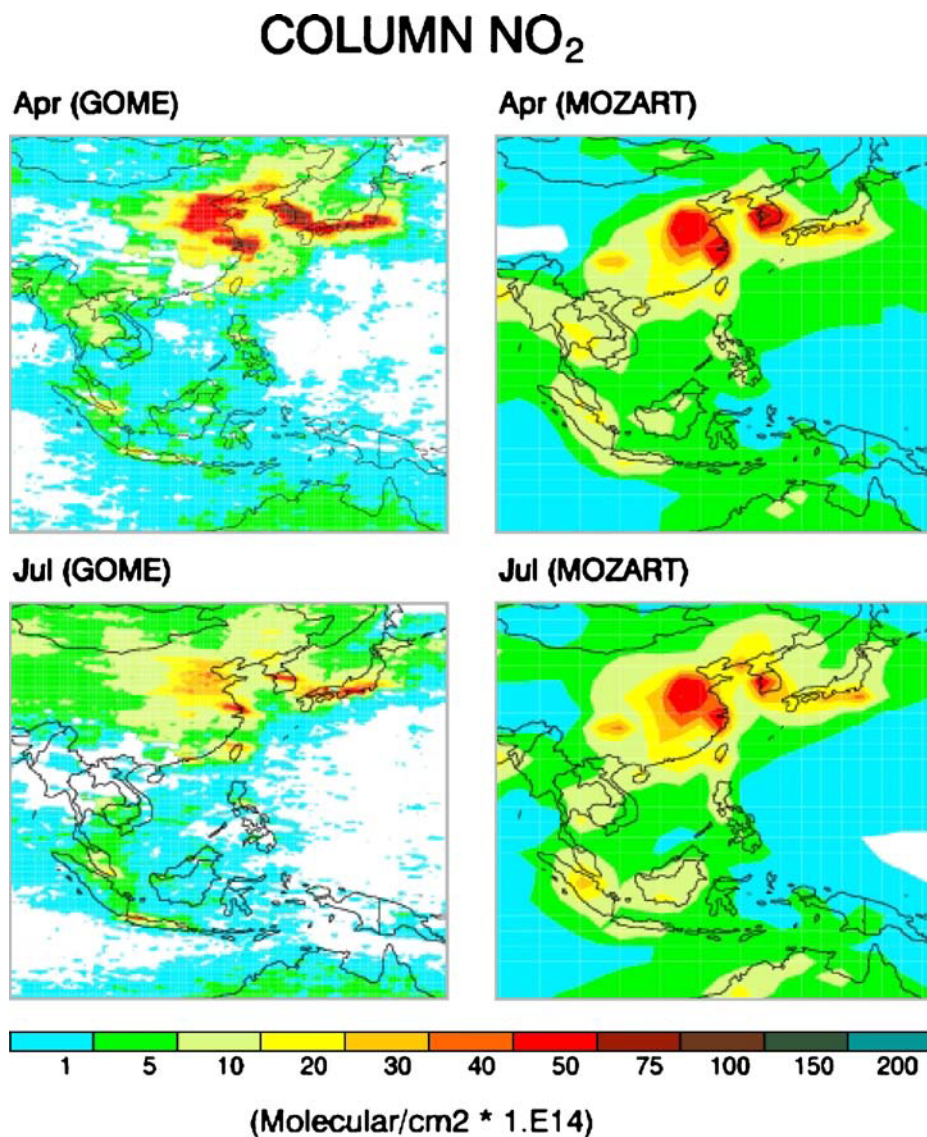
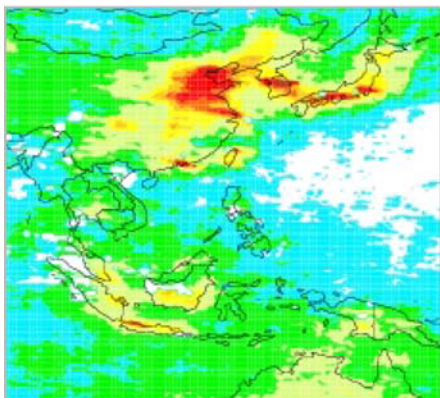


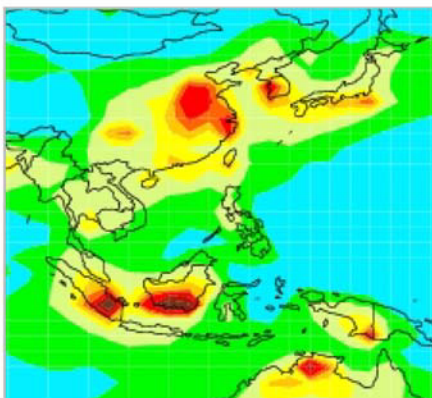
Figure 2 The GOME measured (*left panels*) and the MOZART-2 calculated TNO_2 (*right panels*) (molecules- $\text{cm}^{-2} \times 10^{14}$) in eastern and southeastern Asia in April, July, September, and November 1997, respectively.

COLUMN NO₂

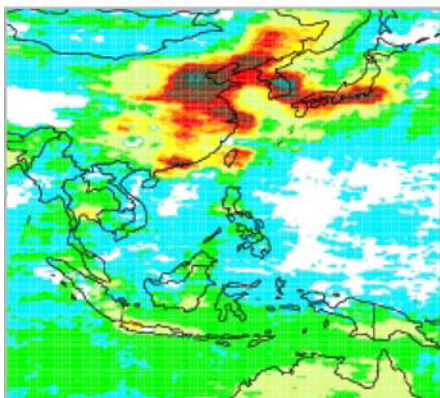
Sept (GOME)



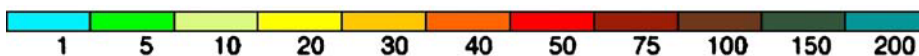
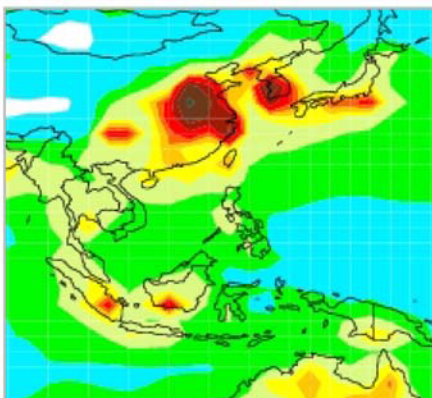
Sept (MOZART)



Nov (GOME)



Nov (MOZART)



(Molecular/cm² * 1.E14)

Figure 2 (Continued).

manifestations of high anthropogenic NO_x emissions in eastern Asia, and are essentially determined by the NO₂ in the planetary boundary layer (PBL). Because the chemical lifetime of NO₂ in the PBL is relatively short (~hours to a day) (Ridley et al. 1996; Tie et al. 2001), the abundance of NO₂ in this region is largely controlled by regional emissions and photochemistry and less by long range transport. NO₂ in this region shows seasonal variations with largest values in November and lowest values in July. The study of Zhao et al. (2006) shows that this strong seasonal feature mainly results from the seasonal variability of the chemical reaction $\text{NO}_2 + \text{OH} \rightarrow \text{HNO}_3$. The chemical resident time of NO₂ due to this reaction varies from a few days in summer to about a month in winter. This results in lower NO₂ in summer and higher NO₂ in winter. Furthermore, there are indications that column

NO₂ is correlated with biomass burning activities in southeastern Asia. For example, in April there are high amounts of TNO₂ in Vietnam and Laos regions ($5\text{--}10\times 10^{14}$ molecules-cm⁻²) when biomass burning activity (i.e., springtime cleanup of vegetation waste) normally occurs. In September high concentrations of TNO₂ are observed in Indonesia ($10\text{--}20\times 10^{14}$ molecules-cm⁻²) which are strongly correlated with large-scale forest fires occurring in September 1997 in this region.

The inferred spatial and seasonal characteristics of TNO₂ from GOME measurements are generally consistent with the model results. For example, the observed elevation in TNO₂ in east-central China, Japan, and South Korea resulting from high industrial activity in these regions is well reproduced by MOZART-2. The strong seasonal variation in MOZART-2 TNO₂ in eastern Asia is also consistent with the measured results. During spring the high TNO₂ values in Vietnam and Laos are very similar to the GOME measurements. The high concentration of TNO₂ in Indonesia in September is also captured in the model calculations. However, discrepancies between model and measurement are also visible. For example, the model TNO₂ is higher in southeastern Asia than the measured values. In east-central Asia the model TNO₂ is somewhat smaller in April and higher in July compared to measurements. In general, the GOME and the modeled column NO₂ differences are within 50% which is within the uncertainty of both GOME measurements and model calculations. Similar differences were also reported by Kunhikrishnan et al. (2004) in their comparison of GOME NO₂ data with the global model of Atmospheric Chemistry and Transport (MATCH-MPIC).

5 Sensitivity of TO₃ and TNO₂ to NO_x Emissions

Comparison of the observed and modeled fields of TO₃ and TNO₂ in Section 4 was limited to spring, summer, and fall months. The winter months were not included because of the poor quality of TCO measurements in these months at middle and high latitudes. This comparison suggests that in spite of some differences, the MOZART-2 model captures the spatial and seasonal characteristics of tropospheric ozone and NO₂ based on satellite measurements. Thus the model provides a valuable tool for analyzing the relative importance of processes contributing to NO_x emissions and their effects on tropospheric ozone in regions of eastern and southeastern Asia.

Three different types of NO_x emissions are selected to conduct this sensitivity study. They are: (1) fossil fuel, (2) biomass burning, and (3) lightning NO_x. The reasons for this selection are: (1) the rapid economical development in Asia, especially China, leading to rapid increase in fossil fuel emissions of NO_x and VOCs, (2) intensive biomass burning activities in southeastern Asia have an important contribution to ozone in this region (there are also often forest fires in Mongolia which lead to high NO_x in northeastern Asia), and (3) lightning emissions have an important impact on tropospheric ozone (Zhang et al. 2003). It is important to understand the relative contribution of lightning NO_x emission in eastern and southeastern Asia. Other NO_x emissions processes, such as aircraft, biofuel emissions (it is relatively small compared to industrial emissions), etc., are not included in this sensitivity study.

The sensitivity of TO₃ to NO_x depends on three major factors: (1) the strength of the emissions, (2) the sensitivity of the ozone formation to VOC and NO_x concentrations (whether it is VOC limited or NO_x limited for the ozone formation in the region), and (3) the seasonal photochemical activities. To illustrate the non-linearity between ozone and

NO_x for tropospheric ozone production, the following reactions regarding the relationship among O_3 , NO_x , and VOCs are discussed. A typical chain of reactions is the following (e.g., Sillman 1995):



If the oxidation of OH by CO or VOCs proceeds quickly through the reactions of R-1 and R-2, it will produce large amounts of HO_2 and RO_2 (radicals produced by VOC oxidations). In this case NO_x will play a significant role in producing O_3 through the reactions of R-4 and R-5. However, if the oxidation of OH by CO or VOCs proceeds slowly, nitric oxide (NO) will react with ozone (R-6) rather than reacting with HO_2 and RO_2 radicals. This will lead to destruction of ozone. In the latter case, ozone production is called ‘VOC limited’ in which ozone production is not sensitive to NO_x concentrations. R-7 and R-8 will terminate the ozone production cycle. From the above analysis, the criteria of ‘VOC limited’ is determined by the ratio between the rates of oxidation of OH by CO or VOCs and the concentrations of total nitrogen. According to the study of Sillman (1995), the ‘VOC limited’ condition can be identified by the ratio of CH_2O (largely produced by the reactions of R-1 and R-2) to NO_y ($\text{NO} + \text{NO}_2 + \text{HNO}_3 + \text{PAN} + \text{NO}_3 + 2\text{N}_2\text{O}_5$). When the ratio of $\text{CH}_2\text{O}/\text{NO}_y$ is less than 0.28, the ozone formation is more sensitive to VOC amounts (i.e., VOC-limited regime). If the ratio is greater than 0.28, ozone formation is sensitive to the NO_x amounts (i.e., NO_x -limited regime). Note that the $\text{CH}_2\text{O}/\text{NO}_y$ ratio is used for afternoon conditions in the study of Sillman (1995). The daily averaged $\text{CH}_2\text{O}/\text{NO}_y$ ratio seems overestimating the VOC-limitation area compared to another indicator of $\text{H}_2\text{O}_2/\text{HNO}_3$ (not shown) suggested by Sillman (1995), indicating that daily averaged value of CH_2O could be smaller than the afternoon value. In the latter case, increases in NO_x emissions lead to an increase in ozone (Kleinman et al. 2001). The VOC limitation could be due to the fact that in China, a large amount of coal burning (five times greater than in the US) and less oil usage (five times smaller than in the US) produce more NO_x than VOC (oil

usage related) emissions. As a result, the ratio of VOC/NO_y is smaller in China than in the US (Tie et al. 2006) and produces a strong VOC-limited condition.

Figure 3 shows the calculated seasonal variation of the ratio of CH₂O/NO_y in eastern and southeastern Asia. In general, the ozone formation is VOC-limited in eastern Asia and NO_x-limited in southeastern Asia. A seasonal variation is also visible for the VOC-limited regions. For example, the VOC-limited regions are larger during April and November than during July and September. During April and November the VOC-limited regions extend from eastern Asia to southern China. Other regions are dominantly NO_x-limited, especially over the Pacific Ocean.

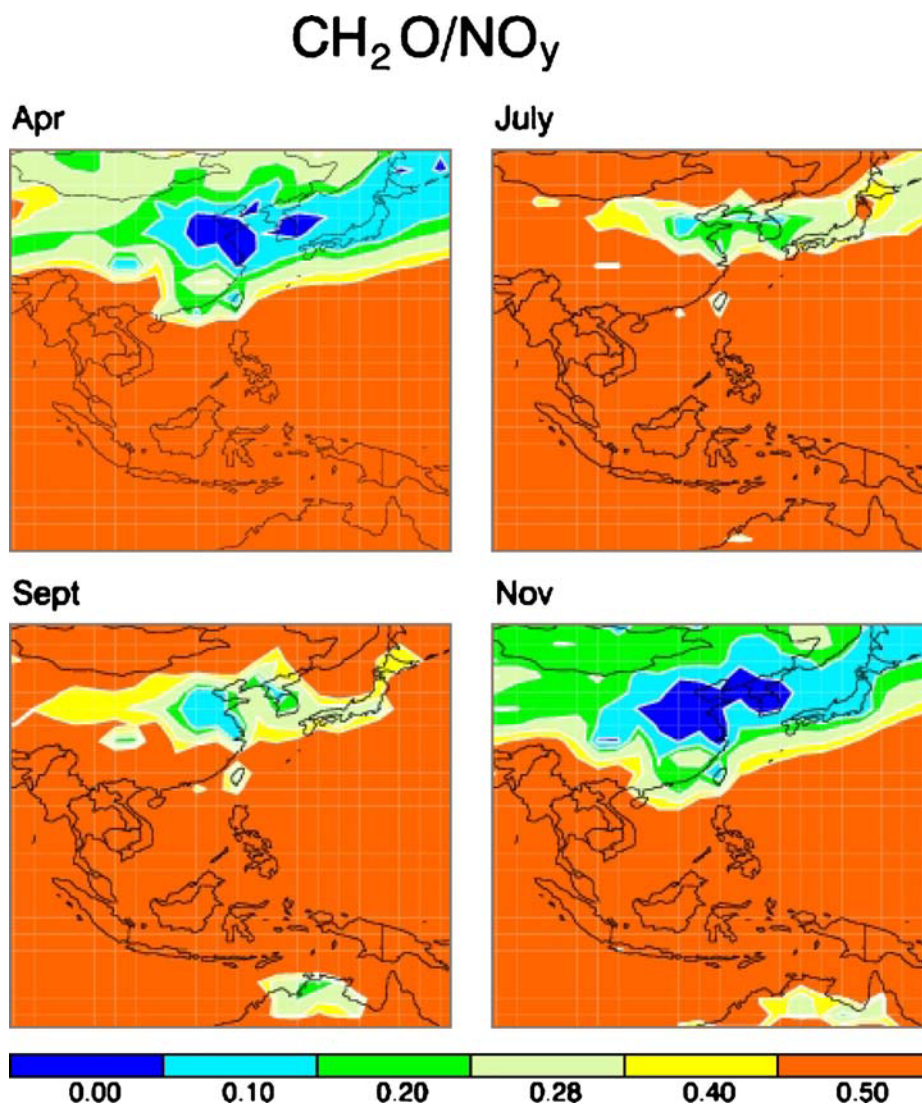


Figure 3 Calculated ratio of CH₂O to NO_y (NO + NO₂ + HNO₃ + PAN + NO₃ + 2N₂O₅) at the surface in eastern and southeastern Asia in April, July, September, and November of 1997, respectively.

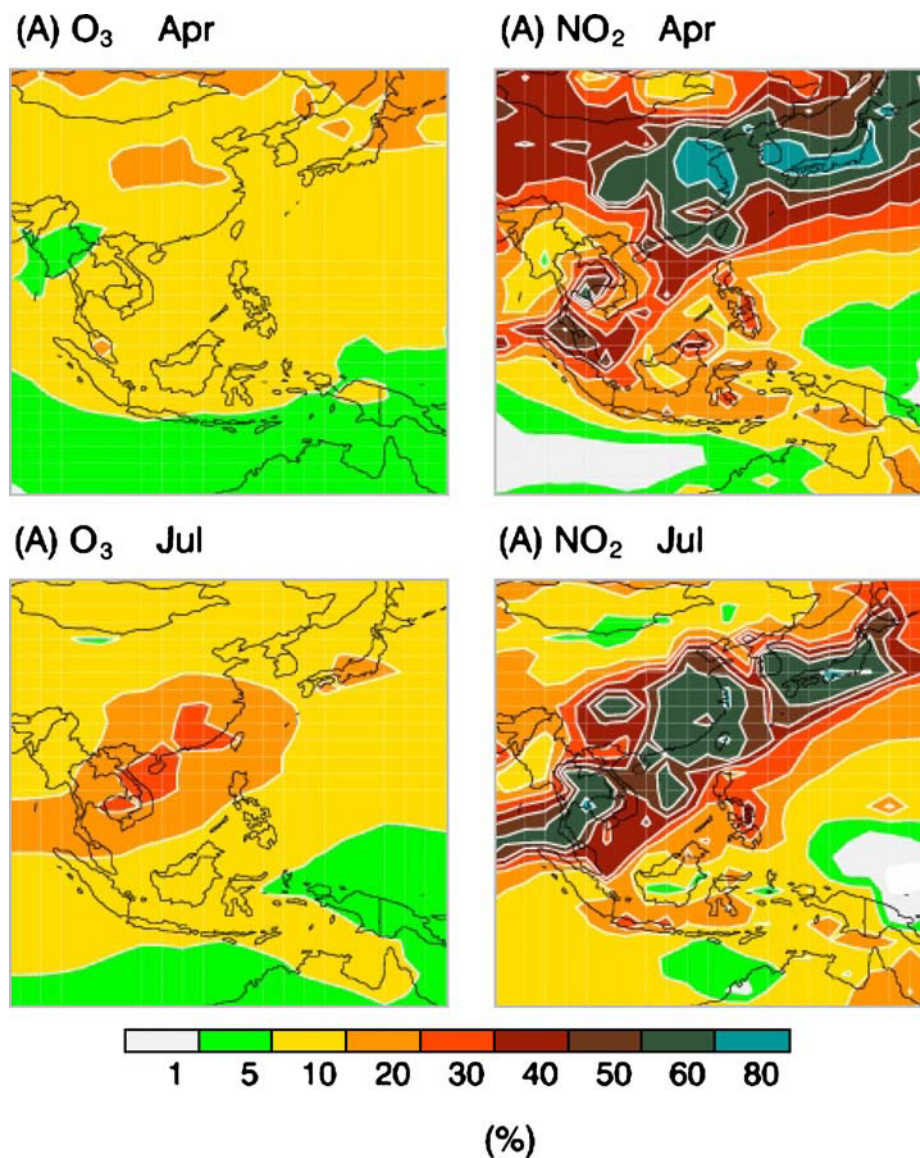


Figure 4 Calculated contribution of fossil fuel NO_x emissions to TO_3 (i.e., the percentage of TO_3 resulting from fossil fuel NO_x emissions).

Within this framework, the MOZART-2 model is used to conduct the sensitivity studies by considering successively the impact of NO_x emissions from fossil fuel, biomass burning and lightning. In each case, each of these emissions was turned on or off, and the impact on the ozone tropospheric column was quantified. In each sensitivity study all other emissions are kept similar. This method differs from the so-called ‘tagged’ tracer method used in some studies (e.g., Lelieveld and Dentener 2000; de Laat et al. 2005). Lelieveld and Dentener (2000) have shown the tagged tracer approach for O_3 essentially yields the same results as

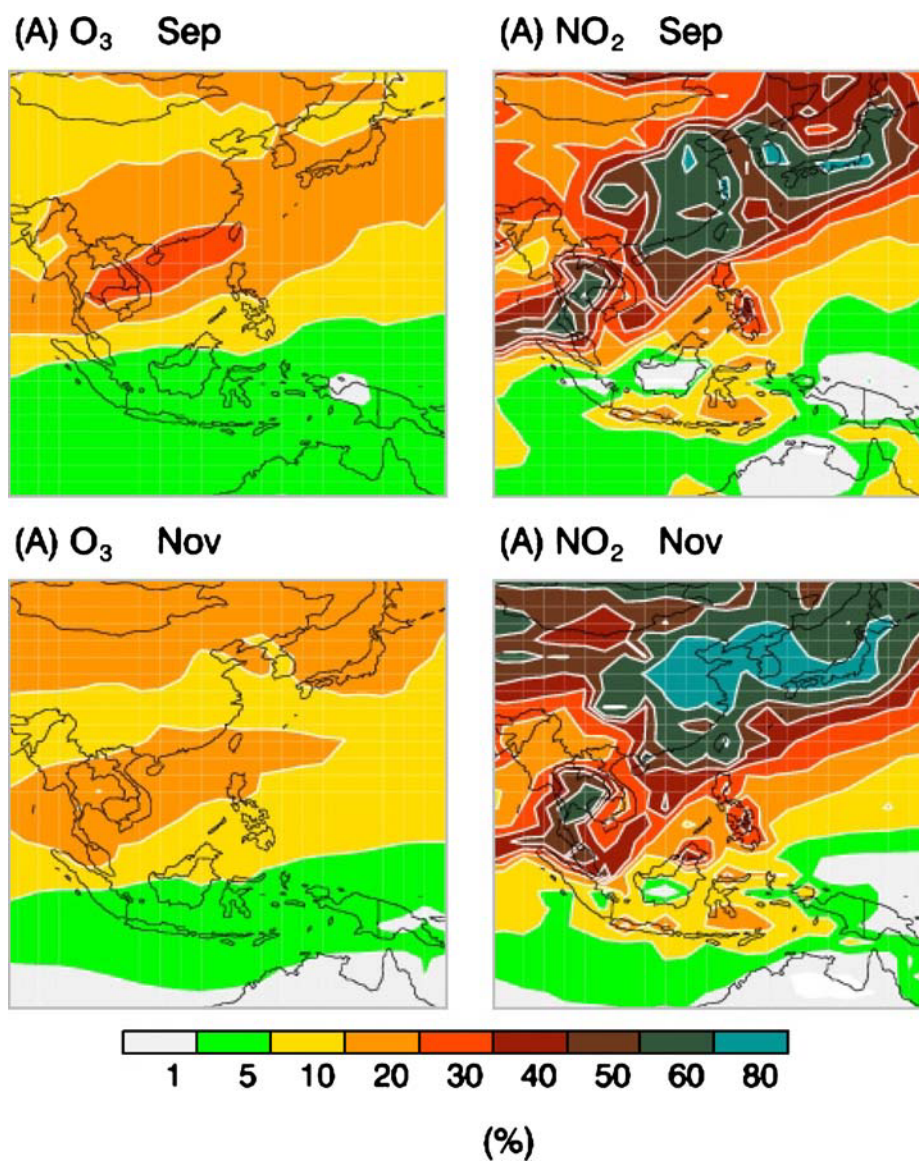


Figure 4 (Continued).

the method based on turning on or off specific sources. It is not clear if the same argument applies for NO_x since the non-linearity effects for NO_x are larger.

5.1 The impact of fossil fuel NO_x emissions on TO_3

Figure 4 shows the effect of fossil fuel NO_x emissions on tropospheric O_3 and NO_2 in terms of percentage change in TNO_2 and TO_3 . In April and November the local fossil fuel NO_x emissions contribute more than 80% to total NO_x in eastern Asia. However, the changes in

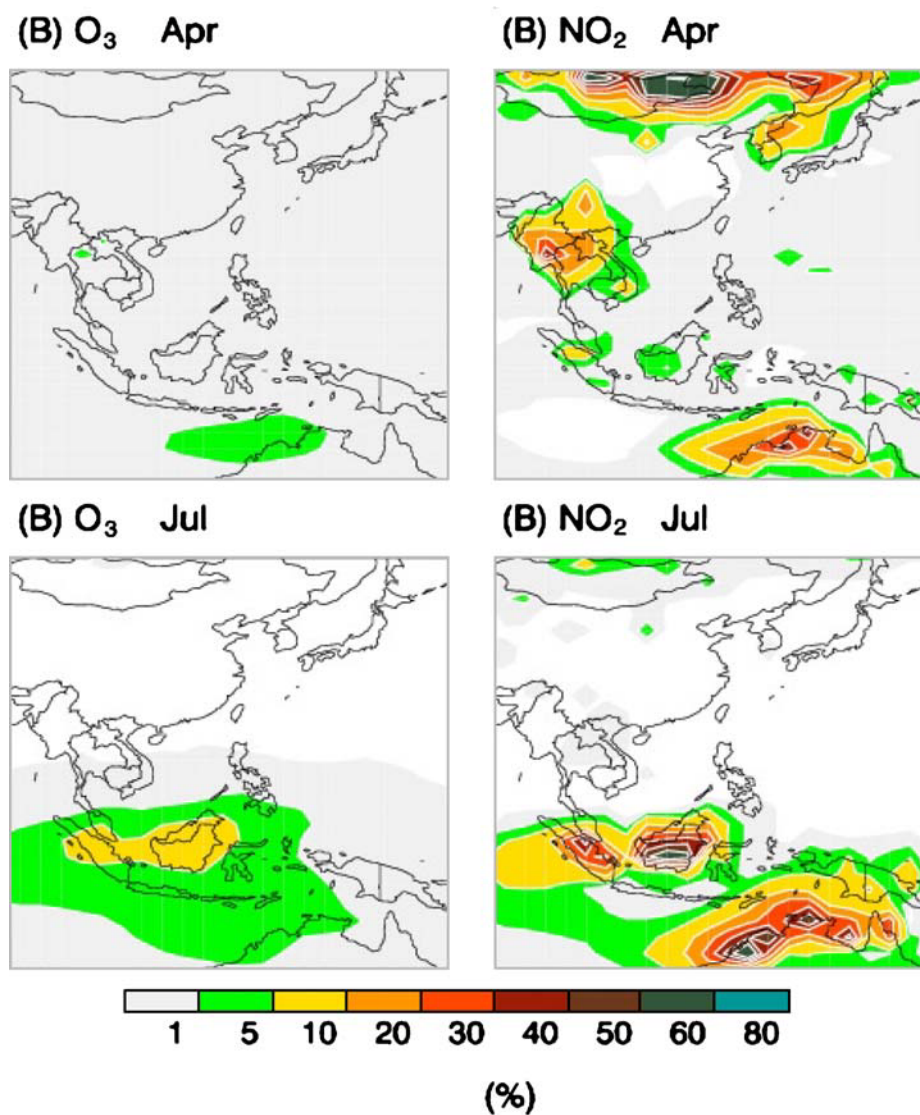


Figure 5 Same as Figure 4 but for biomass burning NO_x emissions.

TO_3 are only about 10%–20%. This region is largely VOC-limited (see Figure 3). As a result, the contribution to TO_3 from fossil fuel NO_x emissions is modest. In July and September the local fossil fuel NO_x emissions contribute about 60% to total NO_x in southeastern Asia. Because this region is largely NO_x -limited (see Figure 3), the resulting changes in TO_3 are larger (20%–30%) than in the VOC-limited region. Likewise, in east-central Asia, although the fossil fuel NO_x emissions contribute more than 60% of total NO_x , the contribution to TO_3 is only about 10%. This is because east-central Asia is a VOC-limited region (see Figure 3). Note that the change of TO_3 in Asia is not only due to the

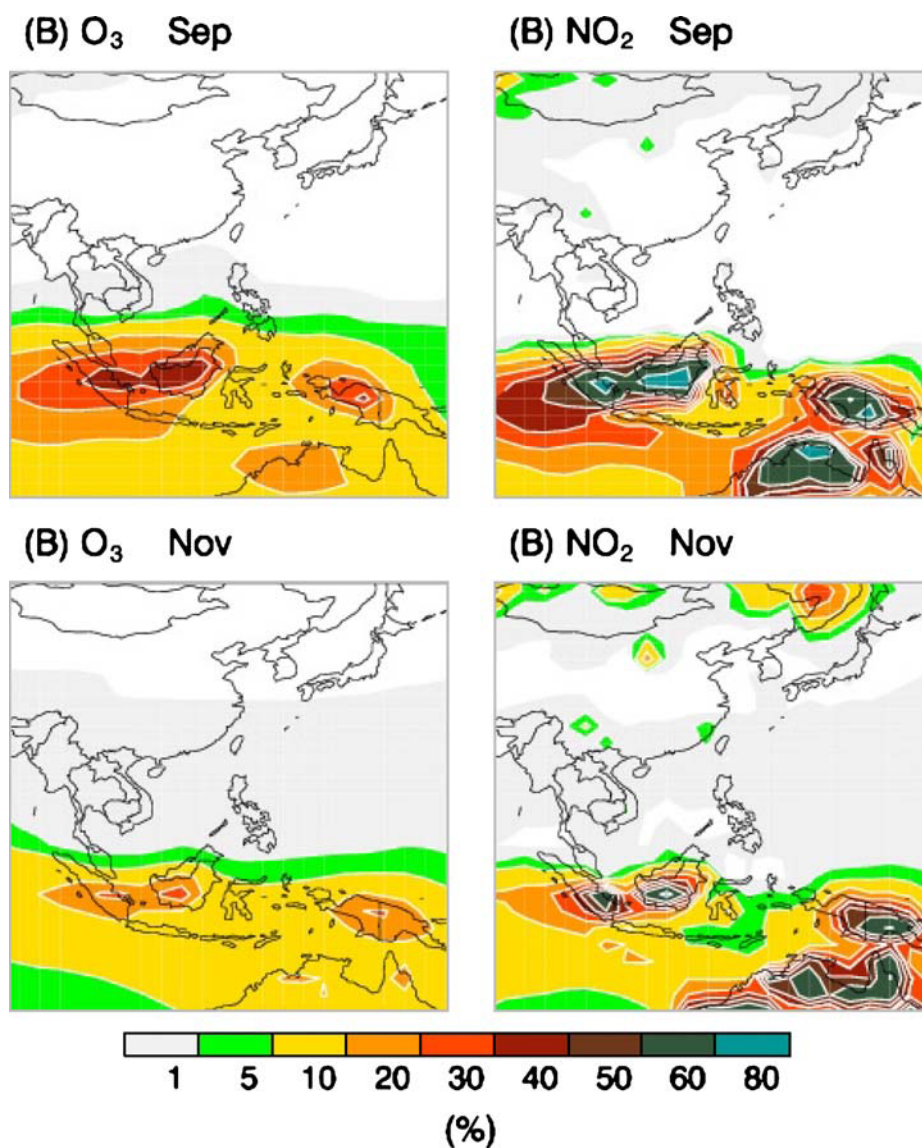


Figure 5 (Continued).

local NO_x emissions, but also due to the long-range transport since the ozone lifetime is about three months in the free troposphere. The seasonal variation of the impact of NO_x on ozone is also due to other factors such as seasonal photochemical activity variation.

5.2 The impact of biomass burning NO_x emissions on TO_3

Figure 5 shows the impact of biomass burning NO_x emissions on TO_3 . In general, the effect of biomass burning NO_x emissions is very small in eastern Asia, and is largest in

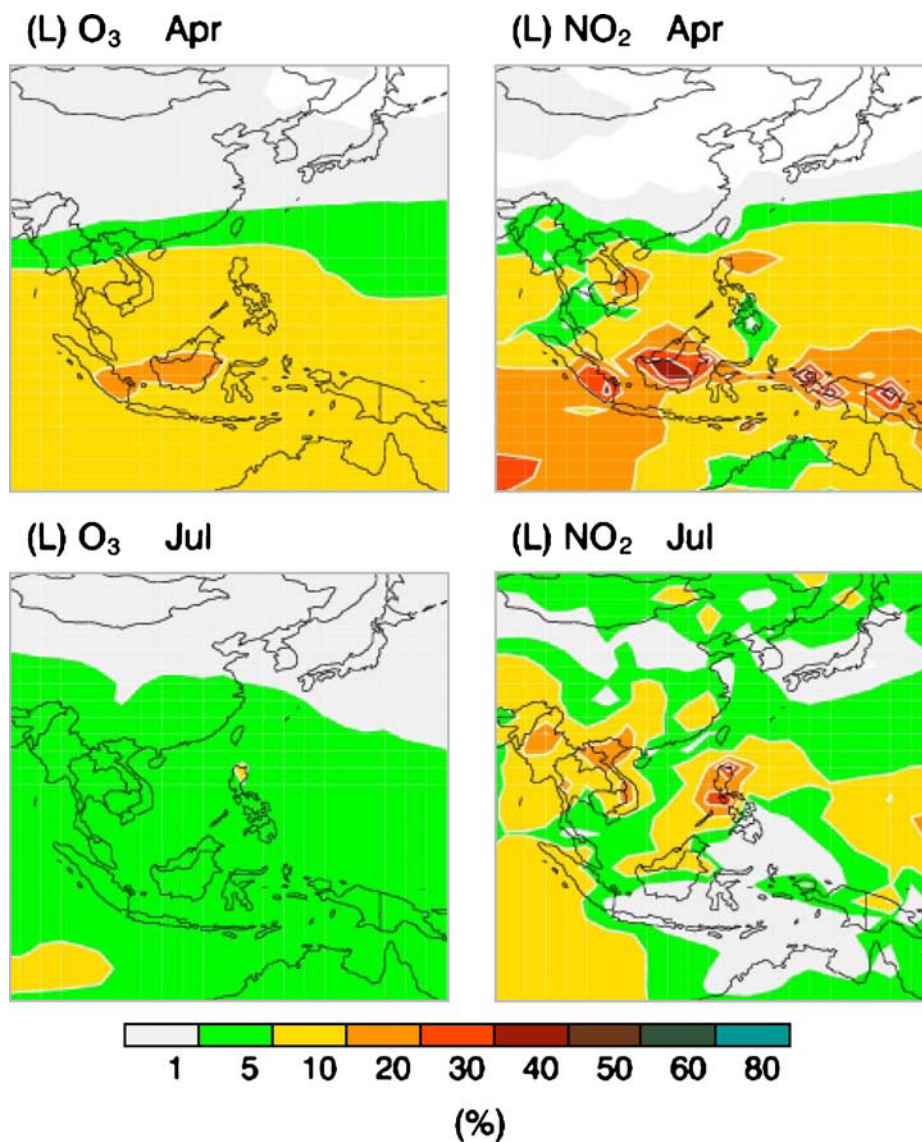


Figure 6 Same as Figure 4 but for lightning NO_x emissions.

southeastern Asia. In April there is an indication that large fires (leading to a significant amount of NO_x emissions) occur in the Mongolian region, and it contributes to about 60% of tropospheric NO_x . However, this biomass burning has little impact on O_3 ozone in the region. This is largely due to the fact that this region is a VOC-limited region (see Figure 3). In July the biomass burning emissions of NO_x in Indonesia contribute about 30%–50% of total tropospheric NO_x , which results in about 10% increase in O_3 in this region. In September 1997 there were extensive forest fires in Indonesia associated with dry conditions induced by El Niño. As a result, total tropospheric NO_x increased by more than

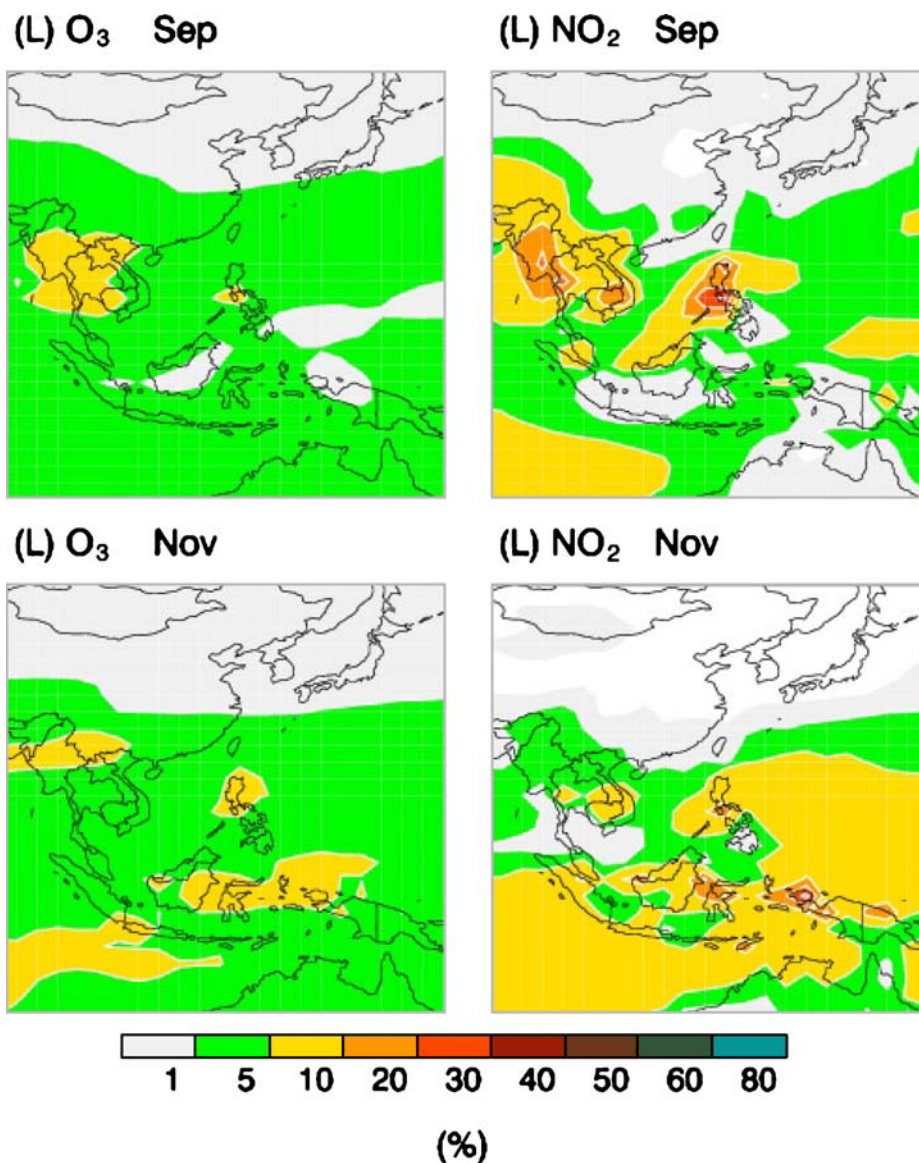


Figure 6 (Continued).

80% and tropospheric column ozone by 30%–40%. In November the biomass burning NO_x emissions in Indonesia were reduced, and corresponding TO_3 concentrations decreased compared to values in September. Note that since the model overestimates TNO_2 of Indonesia fires, the calculated TO_3 resulted from the Indonesia fires could be also overestimated. It may be noted that the El Nino-related increase in TO_3 in 1997 compared to a non-El Nino year were caused by both changes in chemical processes associated with the increase in biomass burning in Indonesia and changes in meteorological conditions. Their relative contributions are almost equal as discussed by Chandra et al. (2002) based on the GEOS-CHEM model.

5.3 The impact of lightning NO_x emissions on TO₃

Figure 6 shows the impact of lightning NO_x emissions on TO₃. In general, the impact of lightning NO_x on ozone is limited mostly to southeastern Asia due to the fact that: (1) Lightning events occur more often in southeastern Asia than in eastern Asia, and (2) southeastern Asia is in the NO_x-limited region. As a result the increase in NO_x concentrations leads to more ozone chemical production than in eastern Asia. In April intense lightning occurs in southeastern Asia, leading to an increase in ozone by about 10%–20% in this region. In July the lightning NO_x emissions shift northward to southern China. As a result the lightning NO_x emission enhances TNO₂ by 10%–20% and TO₃ by about 5% in this region. In September and November there was an increase in TNO₂ of about 10%–20% in southeastern Asia and a corresponding increase of about 5%–10% in TO₃ in that region. In summary, the lightning NO_x emissions have an important impact on O₃ in southeastern Asia including southern China, but it has a small effect on O₃ in regions north of 30°N latitude. Since the lightning NO_x emission is highly parameterized (Horowitz et al. 2003), large uncertainty is associated in estimating its impact on O₃ concentrations in this region.

6 Summary and Conclusions

In this paper we have studied the seasonal and spatial characteristics of tropospheric column O₃ and NO₂ in eastern and southeastern Asia using TOMS/MLS and GOME data, and compared them with the MOZART-2 model. Our study shows generally good agreement between the observed and modeled results within the uncertainties of the measurements and model. The MOZART-2 model captures most of the observed features of TO₃ fields including seasonal variability. For example, the observed plume structure of ozone emanating from industrial regions of eastern China and Japan and traversing over the Pacific Ocean is well simulated by the model. This plume is particularly strong in summer with TO₃ values in the 50–60 DU range. Both the observations and model show elevated values of TO₃ (~35–40 DU) in the Indonesian region in September associated with the 1997 Indonesian forest fires. Both the model and observations show a change in seasonal characteristics of TO₃ from south to north with spring (April) maximum over subtropical latitudes (10–25°N) and summer maximum at higher latitudes.

The model also simulates many of the basic features of the TNO₂ field inferred from the GOME measurements. For example, the high TNO₂ values ($20\text{--}50 \times 10^{14}$ molecules-cm⁻²) in central eastern China, Japan, and South Korea, and their seasonal variations inferred from GOME measurements are comparable to model results. The model captures the general characteristics of TNO₂ in Southeast Asia, e.g., high spring values of TNO₂ in Vietnam and Laos and the El Nino-related increase in September 1997 over the Indonesian region. However, the model values tend to be higher than the values derived from GOME.

Based on these comparisons, we have used the MOZART-2 model to conduct a sensitivity study involving three sources of NO_x emission. They are: (1) fossil fuel, (2) biomass burning, and (3) lightning. The fossil fuel is the major source of NO_x in eastern Asia. However, its effect on tropospheric column ozone is relatively small. In Southeast Asia, the biomass burning and lightning are the major sources of NO_x and have a significant effect on tropospheric column ozone. The varying effects of NO_x on tropospheric column ozone are attributed to differences in relative abundance of volatile organic compounds (VOCs) with respect to total nitrogen in the two regions.

In comparing the model results with satellite data, we restricted the analysis to only few months in spring, summer, and fall seasons because of the orbital characteristics of the UARS satellite, the poor coverage of the MLS measurements in 1997, and increased uncertainty in TOMS/MLS TCO at higher latitudes in winter months. The accuracy of the NO₂ columns was limited by a relatively large footprint (40 by 320 km²) of GOME measurement, and several algorithmic issues related to the assumptions of air mass factor and zonal homogeneities of stratospheric column of NO₂. Both tropospheric ozone and NO₂ are currently being measured from OMI and MLS instruments on the Aura satellite launched recently in July 2004 Ziemke et al. (2006; Bucsele et al. 2006). The new measurements have better global coverage and are not affected by some of the problems associated with TOMS/MLS and GOME measurements. The use of these data in evaluating MOZART-2 and other global models should further improve our understanding of the processes affecting tropospheric ozone.

Acknowledgments We wish to thank James Greenburg for helpful discussions. Funding for this research was provided by Goddard Earth Science Technology (GEST) grant NCC5-494. NCAR is operated by the University Corporation for Atmospheric Research under the sponsorship of the National Science Foundation.

References

- Bond, D.W., Steiger, S., Zhang, R., Tie, X., Orville, R.: The important of production by lightning in the tropics. *Atmos. Environ.* **36**, 1509–1519 (2002)
- Bucsele E.J., Celarier, E.A., Wenig, M.O., Gleason, J.F., Veeffkind, J.P., Boersma, K.F., Boersma, E.: Algorithm for NO₂ vertical column retrieval from the Ozone Monitoring Instrument. *IEEE Trans. Geosci. Remote Sens.* **44** (2006)
- Burrows, J.P., et al.: The Global Ozone Monitoring Experiment (GOME): mission concept and first scientific results. *J. Atmos. Sci.* **56**, 151–175 (1999)
- Chandra, S., Ziemke, J.R., Min, W., Read, W.G.: Effects of 1997–1998 El Nino on tropospheric ozone and water vapor. *Geophys. Res. Lett.* **25**, 3867–3870 (1998)
- Chandra, S., Ziemke, J.R., Bhartia, P.K., Martin, R.V.: Tropical tropospheric ozone, implications for dynamics and biomass burning. *J. Geophys. Res.* **107**(D18), 4351, <http://dx.doi.org/10.1029/2001JD001480> (2002)
- Chandra, S., Ziemke, J.R., Martin, R.V.: Tropospheric ozone at tropical and middle latitudes derived from TOMS/MLS residual: Comparison with a global model. *J. Geophys. Res.* **108**(D9), 4291, <http://dx.doi.org/10.1029/2002JD002912> (2003)
- Chandra S., Ziemke, J.R., Tie, X., Brasseur, G.: Elevated ozone in the troposphere over the Atlantic and Pacific oceans in the Northern Hemisphere. *Geophys. Res. Lett.* **31**, L23102, <http://dx.doi.org/10.1029/2004GL020821> (2004)
- Crutzen, P.J.: Influence of nitrogen oxides on atmospheric ozone content. *Q. J. R. Meteorol. Soc.* **96**(408), 320– (1970)
- de Laat, A.T.J., Aben, I., Roelofs, G.J.: A model perspective on total tropospheric O₃ column variability and implications for satellite observations. *J. Geophys. Res.* **110**, D13303, <http://dx.doi.org/10.1029/2004JD005264> (2005)
- Granier, C., Lamarque, J.F., Mieville, A., Muller, J.F., Olivier, J., Orlando, J., Peters, J., Petron, G., Tyndall, G., Wallens, S.: POET, a database of surface emissions of ozone precursors. Available at <http://www.aero.jussieu.fr/projet/ACCENT/POET.php> (2005)
- Hauglustaine, D.A., Brasseur, G.P., Levine, J.S.: A sensitivity simulation of tropospheric ozone changes due to the 1997 Indonesian fire emissions. *Geophys. Res. Lett.* **26**(21), 3305–3308 (1999)
- Horowitz, L.W., Walters, S., Mauzerall, D., Emmons, L., Rasch, P., Granier, C., Tie, X., Lamarque, J.F., Schultz, M., Brasseur, G.: A global simulation of tropospheric ozone and related tracers: description and evaluation of MOZART, version 2. *J. Geophys. Res.* **108**(D24), 4784, <http://dx.doi.org/10.1029/2002JD002853> (2003)

- Jacob, D.J., Logan, J.A., Murti, P.P.: Effect of rising Asian emissions on surface ozone in the United States. *Geophys. Res. Lett.* **26**(14), 2175–2178 (1999)
- Kleinman, L.I., Daum, P.H., Lee, Y.N., Nunnermacker, L.J., Springston, S.R., Weinstein-Lloyd, J., Rudolf, J.: Sensitivity of O₃ production rate to O₃ precursors. *Geophys. Res. Lett.* **28**(15), 2903–2906 (2001)
- Kunhikrishnan, T., Lawrence, M.G., von Kuhlmann, R., Richter, A., Ladstätter-Weißmayer, A., Burrows, J.P.: Analysis of tropospheric NO_x over Asia using the model of atmospheric transport and chemistry (MATCH-MPIC) and GOME-satellite observations. *Atmos. Environ.* **38**, 581–596 (2004)
- Lelieveld, J., Dentener, F.J.: What controls tropospheric ozone? *J. Geophys. Res.* **105**, 3531–3552 (2000)
- Olivier, J., Peters, J., Granier, C., Petron, G., Müller, J.F., Wallens, S.: Present and future surface emissions of atmospheric compounds. POET report #2, EU project EVK2-1999-00011 (2003)
- Reber, C.A.: The upper Atmosphere Research Satellite (UARS). *Geophys. Res. Lett.* **20**, 1215–1218 (1993)
- Richters, A., Burrows, J.P.: Tropospheric NO₂ from GOME measurements. *Adv. Space Res.* **29**(11), 1673–1683 (2002)
- Ridley, B.A., Dye, J.E., Walega, J.G., Zheng, J., Grahek, F.E., Rison, W.: On the production of active nitrogen by thunderstorms over New Mexico. *J. Geophys. Res.* **101**(D15), 20, 985–21,006 (1996)
- Seinfeld, J.H., Pandis, S.N.: *Atmospheric Chemistry and Physics*. Wiley, New York (1998)
- Sillman, S.: The use of NO_y, H₂O₂, and HNO₃ as indicators for ozone-NO_x-hydrocarbon sensitivity in urban locations. *J. Geophys. Res.* **100**, 14, 175–14,188 (1995)
- Sudo, K., Takahashi, M.: Simulation of tropospheric ozone changes during 1997–1998 El Niño: meteorological impact on tropospheric photochemistry. *Geophys. Res. Lett.* **28**, 4091–4094 (2001)
- Tie, X., Brasseur, G., Zhang, R., Emmons, L., Lei, W.: Effects of lightning on reactive nitrogen and nitrogen reservoir species in the troposphere. *J. Geophys. Res.* **106**, 3167–3178 (2001)
- Tie, X., Brasseur, G., Zhao, C., Granier, C., Massie, S., Qin, Y., Wang, P.C., Wang, G.L., Yang, P.C.: Chemical characterization of air pollution in eastern China and the eastern United States. *Atmos. Environ.* **40**, 2607–2625 (2006)
- Thompson, A.M.: The oxidizing capacity of the Earth's atmosphere – probable past and future changes. *Science* **256**(5060), 1157–1165 (1992)
- Thompson, A.M., Witte, J.C., Hudson, R.D., Guo, H., Herman, J.R., Fujiwara, M.: Tropical tropospheric ozone and biomass burning. *Science* **291**(551), 2128–2132 (2001)
- Valks, P.J.M., PETERS, P.J.M., Lambert, J.C., Zehner, C., Kelder, H.: A fast delivery system for the retrieval of near real-time ozone columns from GOME data. *Int. J. Remote Sens.* **24**(3), 423–436 (2003)
- Velders, et al.: Global tropospheric NO₂ column distributions: comparing three-dimensional model calculations with GOME measurements. *J. Geophys. Res.* **106**(D12), 12, 643–12,660 (2001)
- Vitousek, P.M., Aber, J.D., Howarth, R.W., Likens, G.E., Matson, P.A., Schindler, D.W., Schlesinger, W.H., Tilman, D.G.: Human alteration of the global nitrogen cycle: sources and consequences. *Ecological Applications*, Tempe, AZ. **7**(3), 737–750 (1997)
- Zhang, R., Tie, X., Bond, D.: Impacts of Anthropogenic and Natural NO_x Sources over the U.S. on Tropospheric Chemistry. *Proc. Nat. Acad. Sci. U. S. A.* **100**, 1505–1509 (2003)
- Zhao, C.S., Tie, X., Wang, G.L., Qin, Y., Yang, P.C.: Analysis of air quality in eastern China and its interaction with other regions of the world. **55**, 189–204, doi: 10.1007/s10874-006-9022-1 (2006)
- Ziemke, J.R., Chandra, S., Duncan, B.N., Froidevaux, L., Bhartia, P.K., Levelt, P.F., Waters, J.W.: Tropospheric ozone determined from Aura OMI and MLS: evaluation of measurements and comparison with the Global Modeling Initiative's Chemical Transport Model. *J. Geophys. Res.* **111**, 1–18, D19303, doi: 10.1029/2006JD007089 (2006)